PNL--8387

DE93 004382

Ferrocyanide Safety Project
Subtask 3.4 Aging Studies
FY 1992 Annual Report

M. A. Lilga
M. R. Lumetta
W. F. Riemath
R. A. Romine
G. F. Schiefelbein

November 1992

Prepared for
Westinghouse Hanford Company
Waste Tank Safety Program
under Contract DE-AC06-76RLO 1830
with the U.S. Department of Energy

Pacific Northwest Laboratory
Richland, Washington 99352

Summary

The Hanford Ferrocyanide Task Team is addressing issues involving ferrocyanide precipitates in single-shell waste storage tanks (SSTs), in particular the storage of waste in a safe manner. This Task Team, composed of researchers from Westinghouse Hanford Company (WHC), Pacific Northwest Laboratory (PNL), and outside consultants, was formed in response to the need for an updated analysis of safety questions about the Hanford ferrocyanide tanks.

The Ferrocyanide Safety Project at PNL is part of the Waste Tank Safety Program led by WHC. The overall purpose of the WHC program, sponsored by the U.S. Department of Energy's Tank Farm Project Office, is to 1) maintain the ferrocyanide tanks with minimal risk of an accident, 2) select one or more strategies to assure safe storage, 3) close out the unreviewed safety question (USQ), and 4) identify ultimate disposal options to be used when waste is removed from the tanks.

This annual report gives the results of the work conducted by PNL in FY 1992 on Subtask 3.4, Aging Studies, which is part of Task 3, Chemical Nature of Ferrocyanide in Wastes. Subtask 3.4 deals with the aging behavior and solubilization of ferrocyanide tank waste sludges in a basic aqueous environment. Investigated were the effects of pH variation, ionic strength, salts present in SSTs, and gamma radiation on solubilization of vendor-prepared $Na_2NiFe(CN)_6$.

Vendor-prepared $Na_2NiFe(CN)_6$ dissolves in aqueous base to give primarily insoluble $Ni(OH)_2$ and soluble $Na_4Fe(CN)_6$. Precipitation of $Ni(OH)_2$ apparently drives the ferrocyanide dissolution. From the gamma pit experiments, the insoluble solids contained more than one iron cyanide species, yet to be identified. The rate of dissolution of $Na_2NiFe(CN)_6$ in aqueous base increases with increasing pH. At pH 14, 95% dissolution is observed after 0.5 h. Addition of 1 *M* Na^+ ions in the form of Na_2SO_4 suppresses dissolution at pH 13, presumably because of a common ion effect. However, 1 *M* Na^+ in the form of SST simulant salts (sodium salts of phosphate, carbonate, nitrate, nitrite, sulfate, and hydroxide) resulted in an enhancement of the rate of solubilization most likely arising from buffering of the solution by phosphate. Even when the solution is not stirred, dissolution is relatively rapid. Approximately 40% of the $Na_2NiFe(CN)_6$ dissolves in 24 h in an unstirred solution containing SST salts.

Gamma radiation does not appear to greatly affect the dissolution reaction. Similar rates were observed in unstirred irradiated and control solutions. A more complex mixture of iron cyanides in the insoluble fraction of the gamma radiation experiments is obtained, suggesting the possibility that an iron cyanide species re-precipitates from solution. Further work is needed to determine the identity of this species.

Solubilization work will continue next fiscal year. In addition, cyanide and ferrocyanide hydrolysis studies will be conducted.

Contents

Figures

Tables

Abbreviations

AA	atomic absorption spectroscopy
BDL	below detection limits
DNFSB	Defense Nuclear Facilities Safety Board
DOE	U.S. Department of Energy
EDS	energy dispersive spectroscopy
EIS	Environmental Impact Statement
ESEM	environmental scanning electron microscopy
GAO	General Accounting Office
IC	ion chromatography
IR	infrared spectroscopy
MS	mass spectrometry
PNL	Pacific Northwest Laboratory
SST	single-shell storage tank at Hanford
TBP	tributyl phosphate
USQ	unreviewed safety question
WHC	Westinghouse Hanford Company
XRD	x-ray diffraction spectroscopy

1.0 Introduction

The research performed for this project is part of an effort that started in the mid-1980s to characterize the materials stored in the single-shell waste storage tanks (SSTs) at the U.S. Department of Energy (DOE) Hanford Site (Burger 1984; Burger and Scheele 1988, 1991; Scheele et al. 1991). The Environmental Impact Statement (EIS) for the SSTs, **Disposal of Hanford Defense High-Level, Transuranic and Tank Wastes** (DOE 1987), projected a worst case exposure scenario for an explosion in a ferrocyanide tank to be a short-term radiation dose of 200 mrem to the public. The worst case exposure scenario determined in a later study by the General Accounting Office (GAO) (Peach 1990) was 1 to 2 orders of magnitude larger than the 1987 EIS. A special Hanford Ferrocyanide Task Team was commissioned in September 1990 to address all technical aspects involving SSTs containing ferrocyanide wastes. In October 1990, Secretary of Energy James D. Watkins announced a Supplemental EIS would be prepared that would contain an updated analysis of the safety questions for the Hanford SSTs (DOE 1990).

The Hanford Ferrocyanide Task Team is composed of technical experts from Westinghouse Hanford Company (WHC), Pacific Northwest Laboratory (PNL)[a], and outside consultants. The Ferrocyanide Task Team reports to the DOE Richland Field Office, Tank Farm Project Office, through the Ferrocyanide Safety Program function within WHC. WHC has primary program responsibility for work performed by PNL.

The work described in this topical report was performed in FY 1992 as part of the Ferrocyanide Tank Safety Project, Task 3 - Chemical Nature of Ferrocyanide in Wastes. Specifically, this report discusses work conducted for Subtask 3.4 - Aging Studies, and deals with the aging behavior and solubilization of ferrocyanide tank wastes. This report is divided into three activities:

1. Preliminary Experiments
2. Dissolution Studies
3. Gamma Pit Dissolution Studies.

The report also includes a background section, conclusions from the FY 1992 work, and a discussion of future work.

(a) Operated for the U.S. Department of Energy by Battelle Memorial Institute under Contract DE-AC06-76RLO 1830.

2.0 Background

Radioactive waste resulting from the production of defense nuclear materials has been stored in underground storage tanks at the Hanford Site since the early 1940s. During this time, new technologies were developed, and waste was transferred among tanks to separate different types of waste and to reduce the need for additional tanks. For example, during the 1950s, additional storage volume was required to accommodate the accumulation of high- and low-level radioactive waste without constructing additional storage tanks. As a result, Hanford scientists developed a technology to scavenge radiocesium from either dissolved wastes or waste liquids already stored in the SSTs. This process involved the precipitation of cesium nickel ferrocyanide. An example of a typical flowsheet is shown in Figure 2.1 (Burger and Scheele 1991). The decontaminated supernate was then pumped to a crib. While providing more storage within the tanks, this process added large quantities of ferrocyanide (about 145 metric tons) to the SSTs.

There were three flowsheets used to scavenge the radiocesium from aqueous wastes. The first was used to treat first-cycle waste from the bismuth phosphate process (T-Plant Flowsheet). This generated about 10% of the total ferrocyanide waste. The second, the so-called U-Plant Flowsheet, treated "metal waste" dissolved in nitric acid after the uranium had been recovered using the tributyl phosphate (TBP) process. The U-Plant Flowsheet produced about 70% of the total ferrocyanide wastes. The third process, the so-called In-Farm Flowsheet, treated the basic "metal waste" stored in the Hanford tanks. This process produced the remaining 20% of the total ferrocyanide waste.

T-Plant and U-Plant Flowsheet-treated waste contained substantial metal concentrations that precipitated when neutralized with sodium hydroxide. The ferrocyanide was thereby diluted, assuming that the solids-settling behaviors of the metals and ferrocyanides were the same. It is anticipated that the T-Plant and U-Plant Flowsheets would have a significantly lower concentration of ferrocyanide than In-Farm Flowsheet waste.

Of the 177 waste storage tanks present on the Site, 149 are SSTs. Records at Hanford show 18 SSTs contain at least 200 kg (1000 g-mol) of ferrocyanide precipitates. The ferrocyanide content of the individual tanks ranges from 200 kg up to possibly 16,600 kg (in Tank BY-104) calculated as the $Fe(CN)_6^{4-}$ anion (Borsheim and Simpson 1991). Other wastes in these tanks probably include significant quantities of sodium nitrate, sodium nitrite, silicates, aluminates, hydroxides, phosphates, sulfates, carbonates, uranium, copper, and calcium in addition to the fission products present from the processing of irradiated fuel.

Ferrocyanide by itself is a stable complex of ferrous ion and cyanide that is considered nontoxic because it does not readily dissociate in aqueous solutions. However, in the laboratory, in the presence of oxidizing materials such as nitrates and/or nitrites, ferrocyanide can be made to explode by heating to temperatures above 280°C or by an electrical spark of sufficient energy (Burger and Scheele 1991). The explosive nature of ferrocyanide in the presence of an oxidizer has been known for decades, but the conditions under which the compound can undergo an uncontrolled exothermic reaction have not been thoroughly studied. Explosion propagation properties for large quantities of the material are unknown, and the effects of moisture content and other diluents (or possible catalysts or initiators) that may be present in the tanks are currently being studied. Because the scavenging

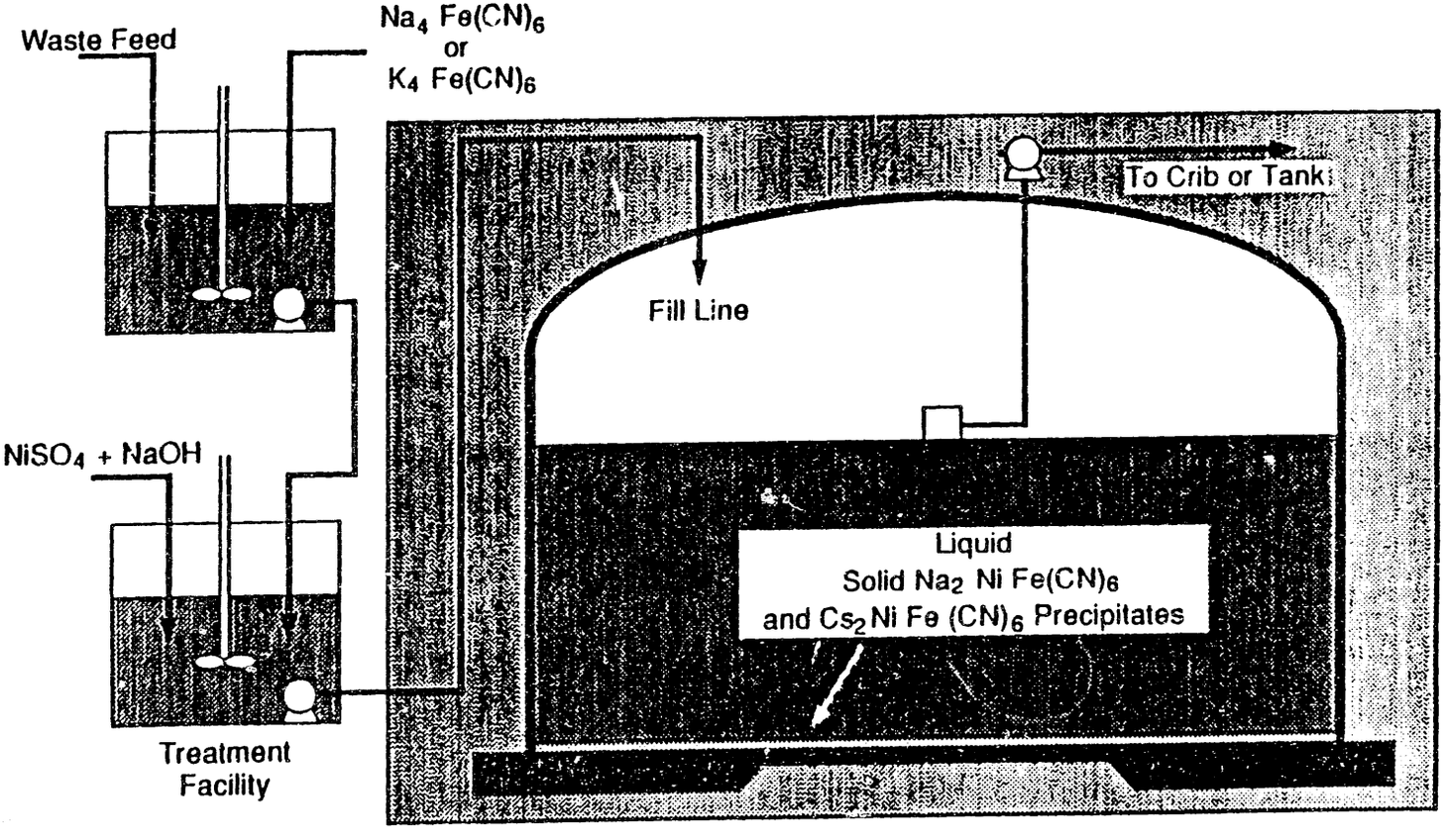

Figure 2.1. Ferrocyanide Scavenging to Remove Cesium

process involved the precipitation of ferrocyanide from solutions containing nitrates and nitrites, it is likely that an intimate mixture of ferrocyanides and nitrates/nitrites exists in parts of some of the SSTs.

The ultimate goal of the work described in this report is to determine the solubility characteristics of simulated ferrocyanide tank wastes in order to obtain a better understanding of the long-term behavior of these wastes and the potential reactivity of the various waste constituents. This work provides baseline data that will be useful when actual SST samples are obtained and analyzed. These results are necessary to answer fundamental questions on the behavior of ferrocyanide wastes in the SST environments and will directly assist in determining: 1) how to maintain the ferrocyanide tanks with minimal risk of an accident, 2) which one or more strategies will assure safe storage, 3) how to close out the unreviewed safety question (USQ), and 4) which ultimate disposal options may be used when waste is removed from the tanks.

3.0 Work Accomplished

The work conducted in FY 1992 for Subtask 3.4, Aging Studies, is discussed below.

3.1 Preliminary Experiments

In the initial dissolution experiments, 1 g of the vendor-prepared material $Na_2NiFe(CN)_6 \bullet Na_2SO_4$[a] $\bullet$ 4.5 H_2O (WHC-2) was refluxed for 96 h in 0.1 *M* (Experiment 1) or 1.0 *M* NaOH (Experiment 2). These experiments were performed in standard laboratory glassware. Table 3.1 summarizes the conditions and results of the two experiments.

Table 3.1. Conditions and Results for Preliminary Experiments

	Experiment 1	Experiment 2
[NaOH]	0.1 *M*	1.0 *M*
Initial pH	12.9	13.8
Final pH	10.5	13.0
$Na_2NiFe(CN)_6 \bullet Na_2SO_4 \bullet 4.5\ H_2O$ (g)	1.0005	1.0041
Moles $Fe(CN)_6^{4-}$ or Ni^{2+}	1.85×10^{-3}	1.86×10^{-3}
Weight of recovered solids (g)	0.3316	0.5113
Solution [Fe] (mg/L)	2030	1600
Moles Fe in solution	1.82×10^{-3}	1.43×10^{-3}
Fraction total Fe in solution	98%	77%
Solution [Ni] (mg/L)	39	3.3
Moles Ni in solution	3.32×10^{-5}	2.81×10^{-6}
Fraction total Ni in solution	1.8%	0.15%
$[NH_3]$ in gas (ppm)	30	375
Approx. moles NH_3 produced	8.04×10^{-8}	2.34×10^{-6}
Approx. %-yield NH_3	0.0007	0.02

Atomic absorption (AA) analysis of the reaction supernates showed that essentially all of the iron is in solution after 96 h at reflux conditions. Very little of the nickel is found in the supernate solutions. Environmental scanning electron microscopy (ESEM) and energy dispersive spectroscopy (EDS) of the soluble solids recovered from the supernate are consistent with the AA results, showing the presence of iron but not nickel. Infrared spectroscopy (IR) and X-ray diffraction (XRD) indicated that $Na_4Fe(CN)_6$ is the primary ferrocyanide compound in the soluble solids.

(a) Unwashed material prepared by Atomergic Chemetals, Corp., Farmingdale, New York, using a sulfate-based flowsheet.

The insoluble solids were characterized by IR, ESEM, EDS, XRD, and Mössbauer analyses. ESEM showed the presence of nickel in the reaction precipitate. Iron was also detected at very low levels. IR and XRD results showed that the nickel-containing insoluble species is $Ni(OH)_2$. In addition, IR and EDS showed the presence of significant quantities of silica, which originates from etching of the Pyrex glassware used in these experiments. The greater weight of the insoluble solids obtained in Experiment 2 (1.0 *M* NaOH) is due to a larger amount of silica etched from the glassware in this sample. For this reason, Teflon labware was used in subsequent experiments. The Mössbauer spectrum of the insoluble solids from the 1.0 *M* NaOH dissolution is weak, indicating a low iron content. Two peaks are observed consistent with the presence of ferrocyanide anion and another unidentified iron-containing species.

The presence of NH_3 was detected in both experiments. This is indicative of cyanide hydrolysis reactions. A greater degree of hydrolysis occurs in the more basic solution. The extent of hydrolysis, however, is very low after 96 h with the largest yield on the order of 0.02% (0.02% of the cyanide groups were converted to NH_3).

In summary, the results of these preliminary experiments indicate that $Na_2NiFe(CN)_6$ reacts with NaOH to form insoluble $Ni(OH)_2$ and soluble $Na_4Fe(CN)_6$ according to:

$$Na_2NiFe(CN)_6 + 2\ NaOH \longrightarrow Na_4Fe(CN)_6 + Ni(OH)_2$$

This reaction appeared to occur rapidly at room temperature in Experiment 2 (1.0 *M* NaOH). The addition of 1.0 *M* NaOH to the ferrocyanide material before heating resulted in an immediate color change. The change was slower when 0.1 *M* NaOH was added.

3.2 Dissolution Studies

Table 3.2 summarizes the experiments performed in this work task. The objectives of this task were to determine the influence of pH, ionic strength, and the presence of SST simulant salts on the rate and total dissolution of the vendor-prepared $Na_2NiFe(CN)_6$ material. The primary difference between these experiments and the preliminary experiments is that these reactions were performed at room temperature in Teflon labware.

3.2.1 pH Variation Experiments

Experiments to study the effect of initial pH on ferrocyanide dissolution were conducted in Teflon labware. The reactions were performed at a starting pH of 12, 13, and 14 (0.01 *M*, 0.1 *M*, and 1.0 *M* NaOH, respectively). Solutions were periodically sampled during the reaction and analyzed for iron by AA. At the conclusion of the experiment, the final pH was measured and the soluble and insoluble solids were analyzed by IR, ESEM, EDS, XRD, and occasionally by Mössbauer spectroscopy. In some cases, the supernate was analyzed for free cyanide, ferrocyanide, and ferricyanide by ion chromatography (IC). Table 3.3 summarizes the starting and final pH for these experiments.

Table 3.2. Summary of Ferrocyanide Solubility Experiments Conducted Using the Vendor-prepared Material (WHC-2), $Na_2NiFe(CN)_6 \bullet Na_2SO_4 \bullet 4.5\ H_2O$

I. pH Variation: pH = 12, 13, 14

II. pH Variation at 1 *M* [Na^+]: pH = 12, 13, 14

III. pH 13 at 1 *M* [Na^+] with Added SST Simulant Salts (Na salts of NO_3^-, NO_2^-, PO_4^{3-}, SO_4^{2-}, CO_3^{2-}, and OH^-)

IV. Static Solubility Test: pH 13, 1 *M* [Na^+], 25°C

V. Gamma Radiation: pH 13 at 1 *M* [Na^+] with Added SST Simulant Salts

Table 3.3. Starting and Final Solution pH in Dissolution Experiments

Experiment	Starting pH	Final pH
pH Variation		
0.01 *M* NaOH	12.0	11.6
0.1 *M* NaOH	12.9	12.4
1.0 *M* NaOH	14.0	13.4
Constant 1 *M* [Na^+]		
0.1 *M* NaOH	12.9	12.4
SST Simulant Salts		
stirred	13.0	13.0
static	13.0	12.9
Gamma Pit		
irradiated	13.0	12.9
control	13.0	12.9

The Teflon labware used in these experiments proved, for the most part, to be impervious to the high pH solutions employed in the dissolution experiments. However, some degradation of the Teflon labware did occur. The small amount of Teflon did not cause a problem in subsequent analyses, because it could easily be removed by skimming the top of the reaction mixture before filtering.

Figure 3.1 is a comparison of the EDS micrographs from the analysis of the soluble and insoluble solids obtained from 1.0 *M* NaOH (pH 14) dissolution of the vendor-prepared $Na_2NiFe(CN)_6$. As observed in the preliminary experiments, nickel is found in the insoluble solids and iron is predominantly found in the soluble solids.

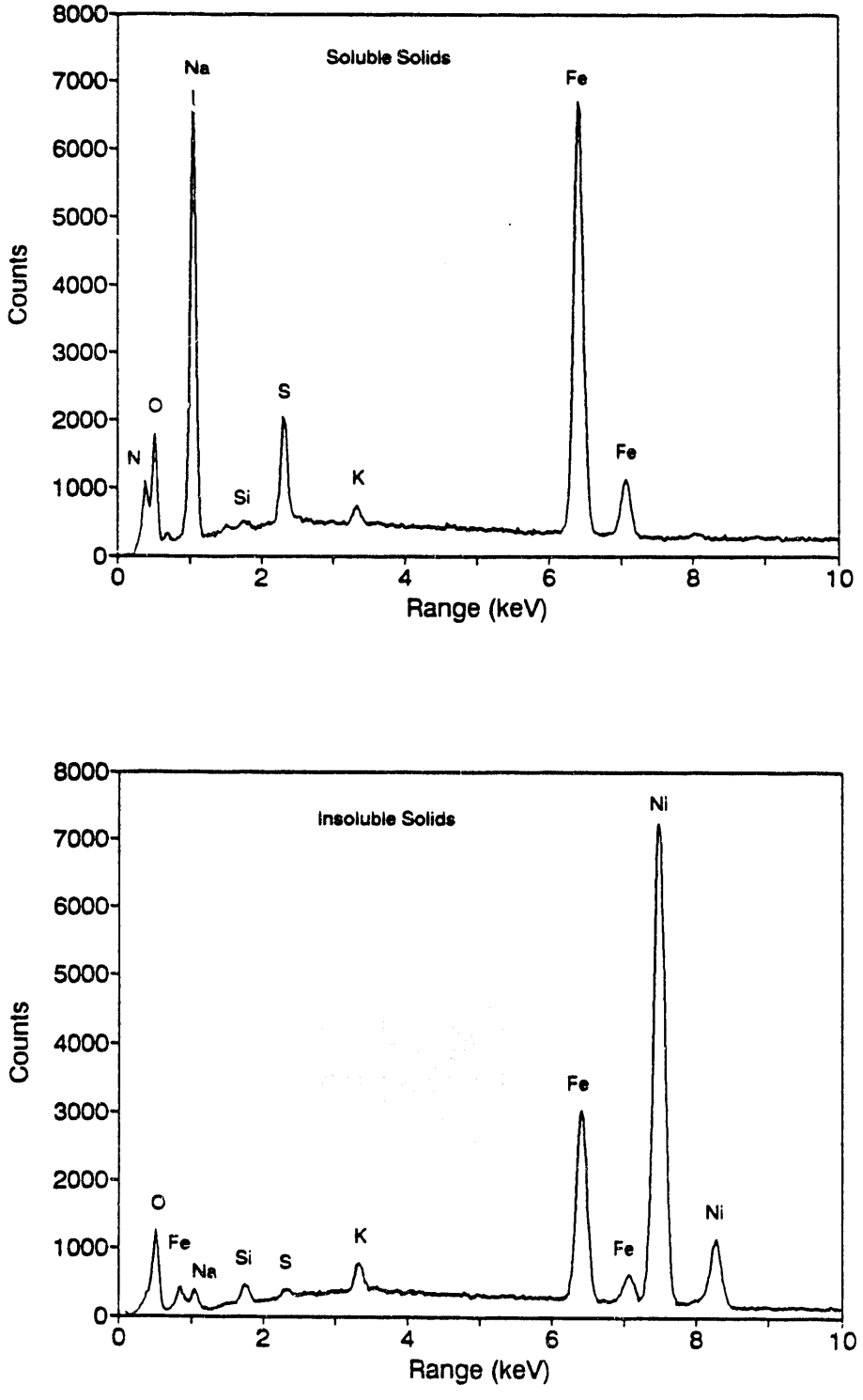

Figure 3.1. Comparison of EDS Micrographs of the Soluble and Insoluble Solids Obtained from pH 13 Dissolution of the Vendor-prepared $Na_2NiFe(CN)_6$

Figure 3.2 compares the XRD results for laboratory-prepared $Ni(OH)_2$ with the soluble and insoluble solids obtained from 1.0 *M* NaOH dissolution of the vendor-prepared $Na_2NiFe(CN)_6$. These data indicate that the insoluble material is probably $Ni(OH)_2$ and that the soluble solids are most likely $Na_4Fe(CN)_6$.

These conclusions are also supported by IR data. Figure 3.3 illustrates the spectral differences in the OH region between the soluble and insoluble solids (for 0.1 *M* and 1.0 *M* NaOH dissolutions) versus the laboratory-prepared $Ni(OH)_2$. The solids obtained from the supernates show broad absorptions for water, while the insoluble solids have an additional sharp band. This band corresponds well with that observed for $Ni(OH)_2$. Figure 3.4 shows the growth of this band in samples taken over the course of the 0.1 *M* NaOH dissolution experiment. The band is not easily resolved until after 24 h reaction time. Infrared spectra in the cyanide region are shown in Figure 3.5 and summarized in Table 3.4. Insoluble reaction products show a peak position consistent with the vendor-prepared starting material, i.e., $Na_2NiFe(CN)_6$. Soluble products display a peak position consistent with $Na_4Fe(CN)_6$.

Mössbauer spectra of the insoluble solids from the 0.1 *M* NaOH dissolution, Figure 3.6, indicate the presence of a single iron-containing species. Similar results were obtained for the soluble material and the starting vendor-prepared material. Spectra are consistent with that of ferrocyanide anion. In contrast to the solids obtained from reflux in 0.1 *M* NaOH (described in Section 3.1), no other iron-containing species are present at a detectable level in these samples.

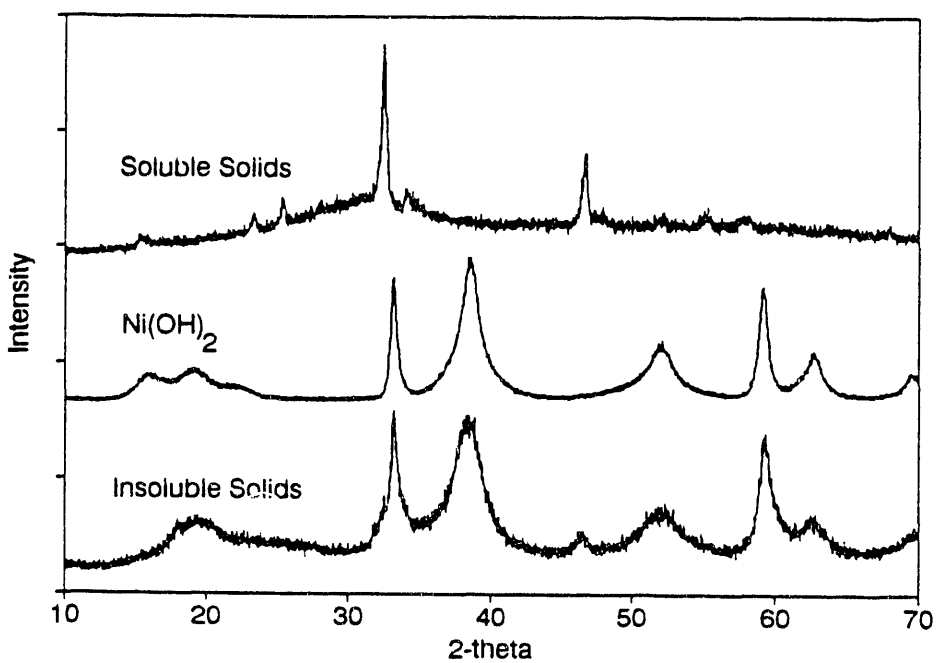

Figure 3.2. Comparison of XRD Results for Laboratory-prepared $Ni(OH)_2$ with the Soluble and Insoluble Solids Obtained from pH 14 Dissolution of the Vendor-prepared $Na_2NiFe(CN)_6$

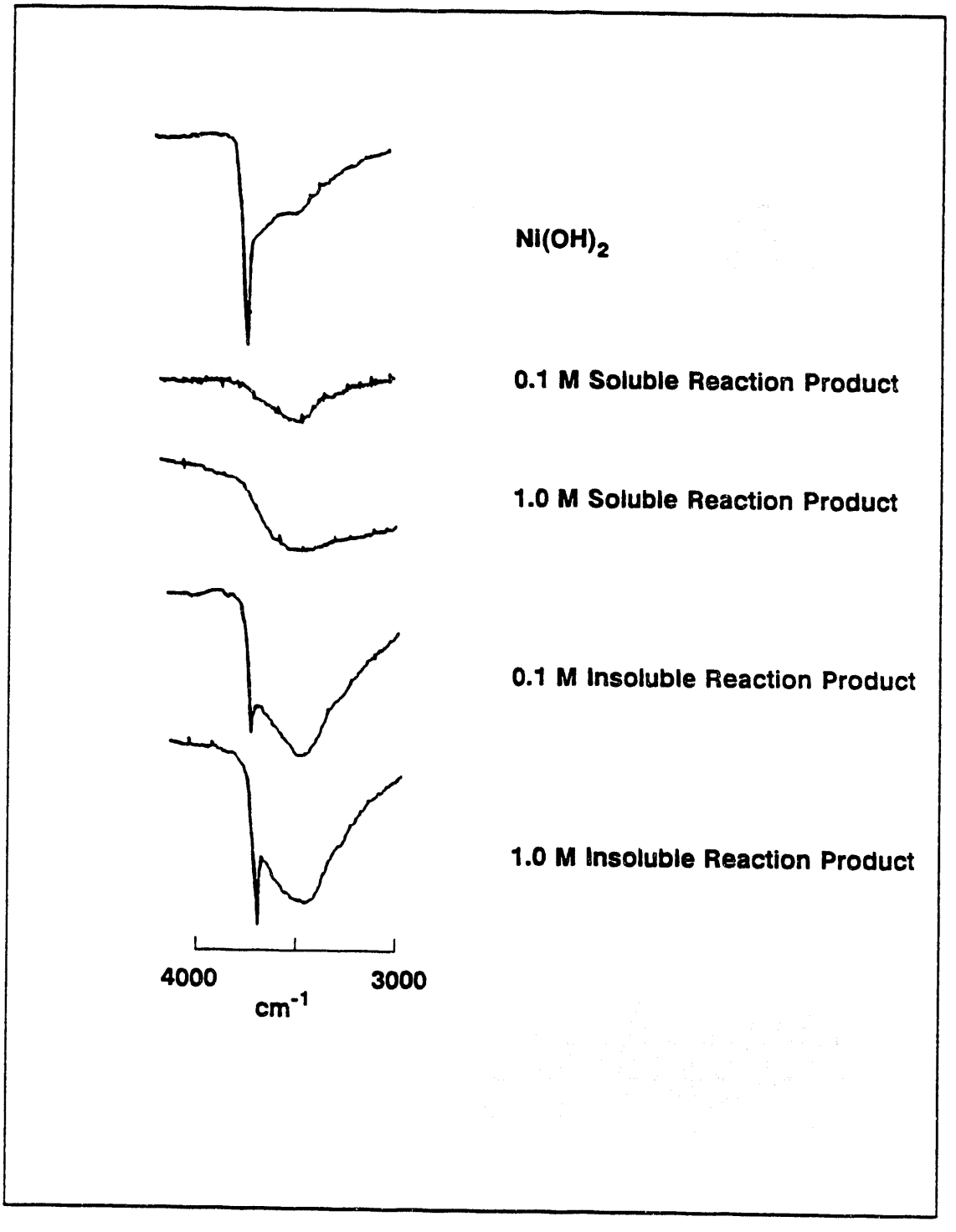

Figure 3.3. Infrared Spectra in the Hydroxyl Region for Dissolution Reaction Products

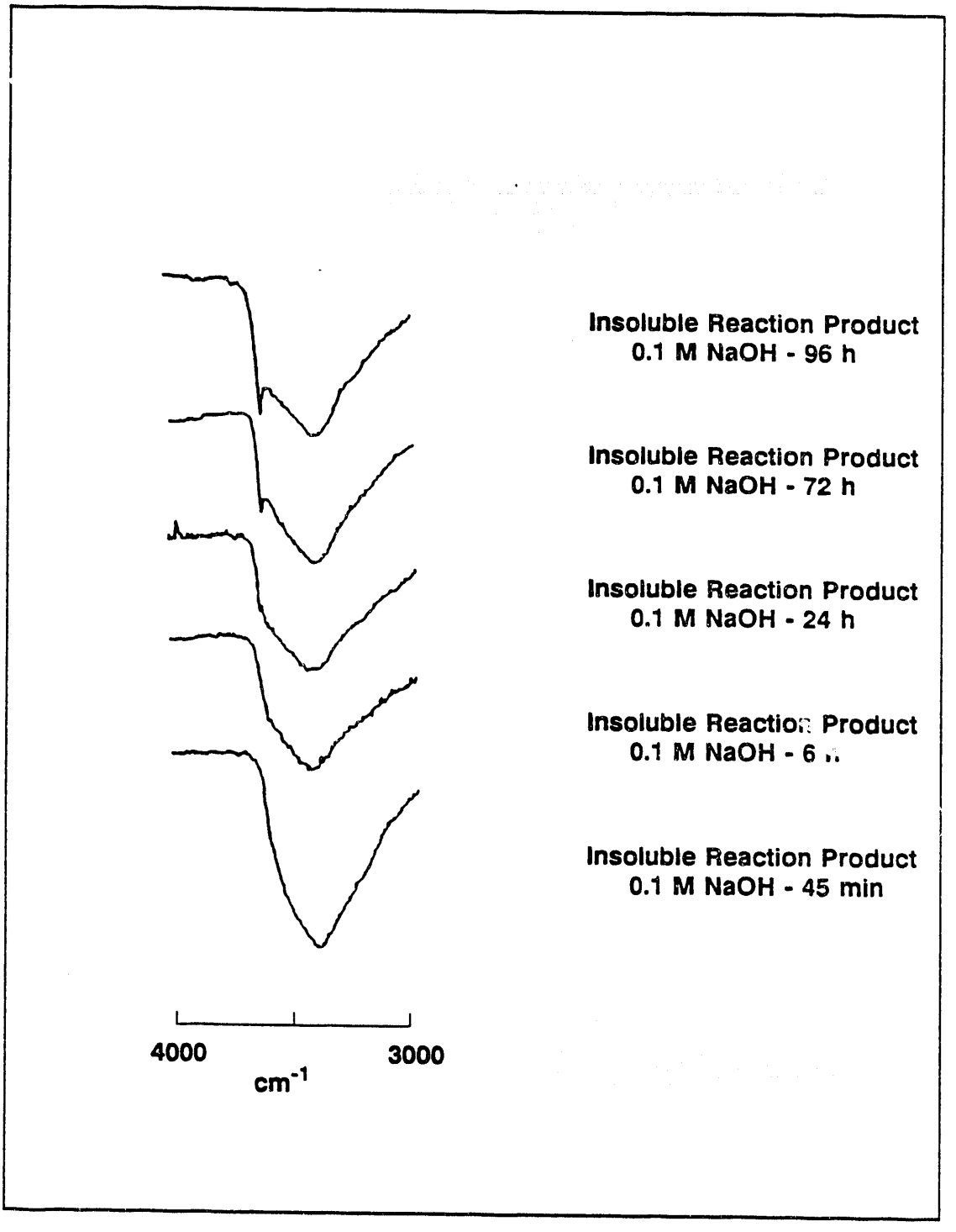

Figure 3.4. Infrared Spectra of Reaction Products in the Hydroxy Region Over Time During Dissolution of Vendor-prepared $Na_2NiFe(CN)_6$ in 0.1 *M* NaOH

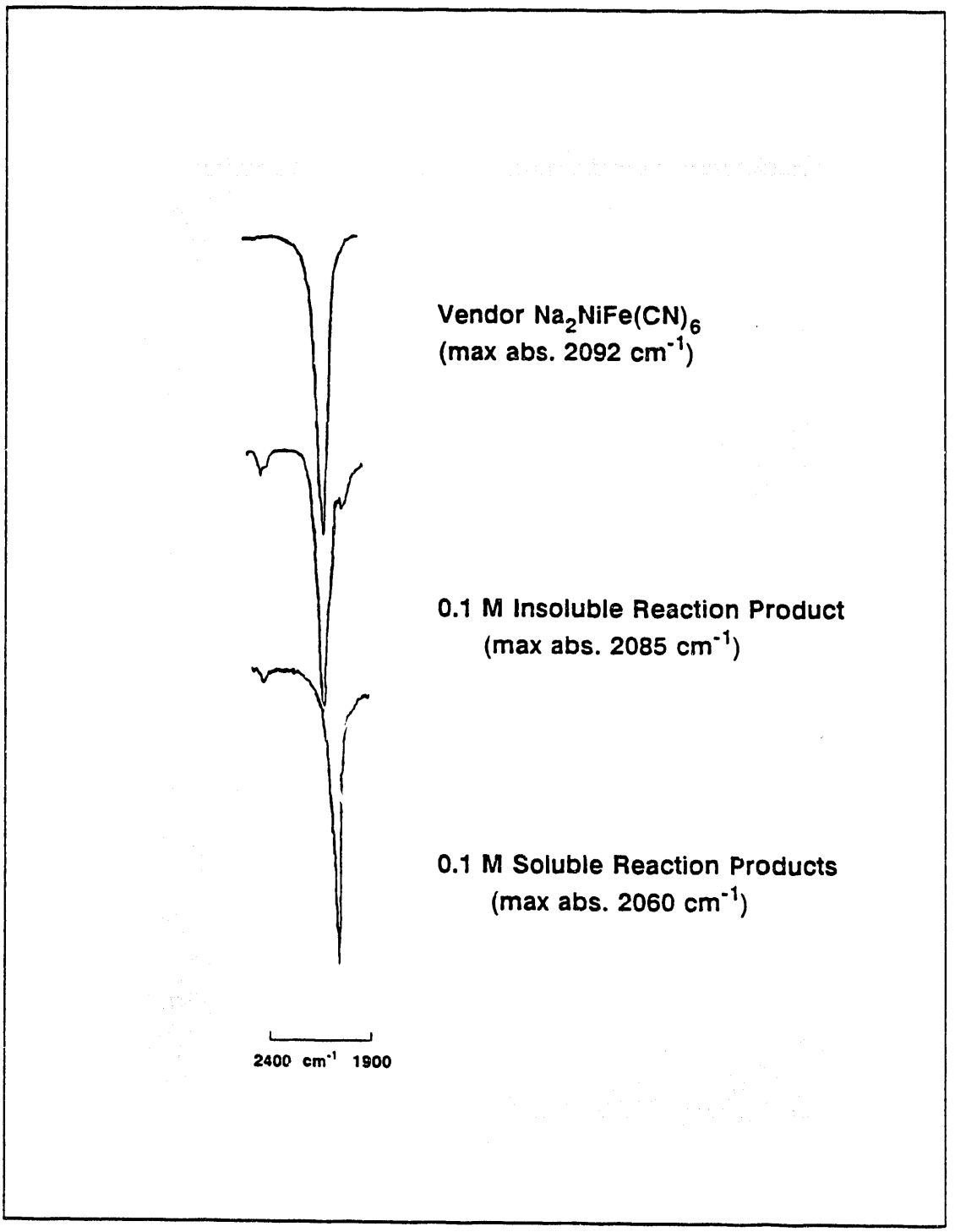

Figure 3.5. Infrared Spectra of Reaction Products in the Region of Cyanide Absorbance

Table 3.4. Infrared Absorbances (cm^{-1}) in the Cyanide Region for Samples in the Solid State[a]

Experiment	Soluble Solids	Insoluble Solids
pH 12	2025w, 2059s	2090
pH 13	2060[b]	2093
pH 14	2024w, 2060s	2089
Gamma Control	2023w, 2054s[b]	2006m, 2025w, 2047s, 2064sh, 2094m
Gamma Irradiated	2025w, 2057s[b]	2008s, 2025w, 2046sh, 2055s, 2094w
Static SST Salts	2025w, 2058s[b]	2003w, 2054sh, 2093s
$Na_2NiFe(CN)_6$[c]	-	2092
$K_4Fe(CN)_6$	2047[b]	-
$Na_3Fe(CN)_5(H_2O)$	2043[d]	-
$K_3Fe(CN)_6$	2125[d]	-

(a) w = weak, m = medium, s = strong, sh = shoulder.
(b) In solution, these materials gave a single absorbance at 2036 cm^{-1}.
(c) Vendor-prepared material.
(d) Nakamoto (1970).

The dissolution of iron into the supernate was monitored by performing AA analysis on supernate samples removed from the reaction mixture at various time intervals. Analyses of the supernates by AA were straightforward for the pH 13 and pH 14 solutions. However, some trouble was encountered with the formation of unfilterable fines on the first attempt using 0.01 *M* NaOH. This problem was most likely caused by the low ionic strength of the pH 12 solution. To overcome this problem, samples were taken from the reaction mixture and mixed with a 0.5 *M* Na_2SO_4 solution. After the samples were mixed for about 30 s in the sample syringe, the fines were easily filtered.

The effect of pH on solubility is shown in Figure 3.7. Dissolution is 95% complete after 0.5 h stirring in 1 *M* NaOH (pH 14) at room temperature. The reaction at pH 12 is base-limited, but the base is rapidly consumed within 0.1 h. At pH 13, a slight excess of base is present; the dissolution proceeds rapidly at first then slows to reach about 85% completion in 144 h, as shown in Figure 3.8. Presumably, the dissolution would continue to completion at longer reaction times at pH 13. IC data on free cyanide in solution in the pH 14 experiment are shown in Figure 3.9. Very little dissociation of free cyanide occurs; the maximum [CN^-] is about 6 ppm (2.31×10^{-4} *M*) compared with about 2000 ppm (3.58×10^{-2} *M*) Fe. The increase in [CN^-] roughly parallels the [Fe] increase as shown in Figure 3.10.

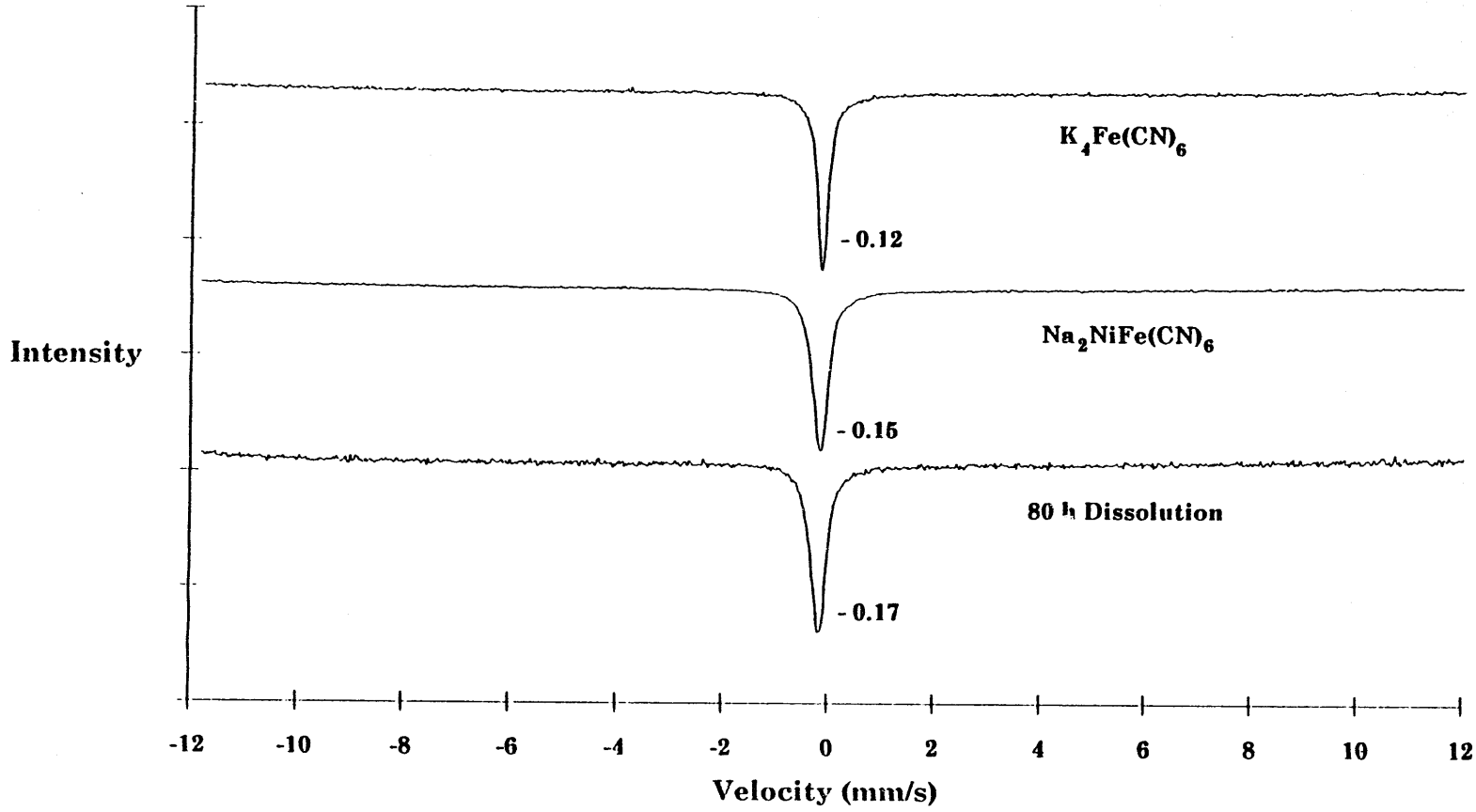

Figure 3.6. Mössbauer Spectra of Ferrocyanide Materials Including Insoluble Solids from 80 h Dissolution in 0.1 *M* NaOH

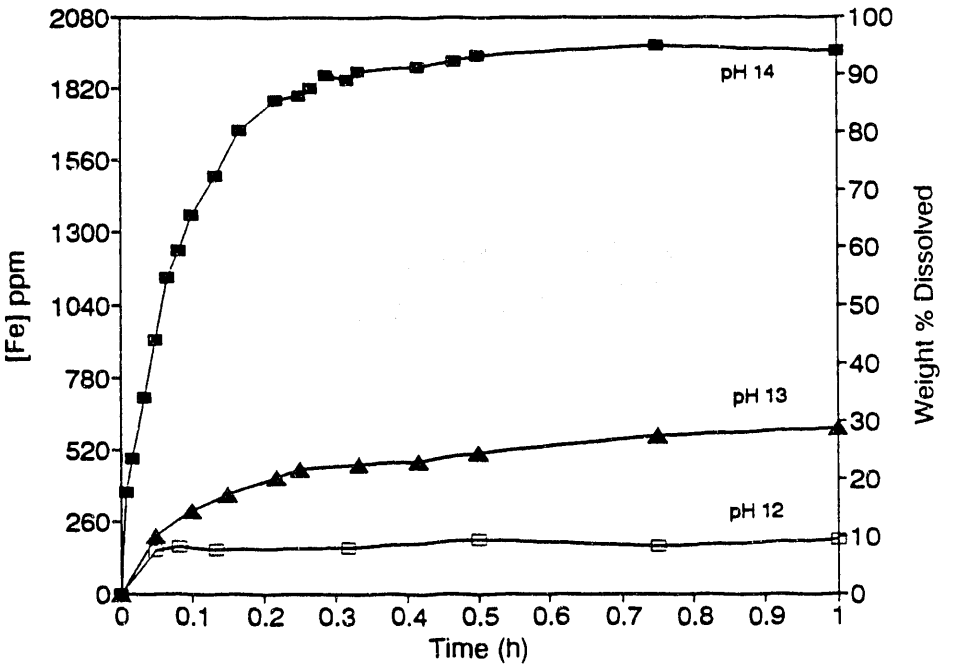

Figure 3.7. Solubility of Vendor-prepared $Na_2NiFe(CN)_6$ in NaOH as a Function of pH at 25°C, First Hour of Dissolution

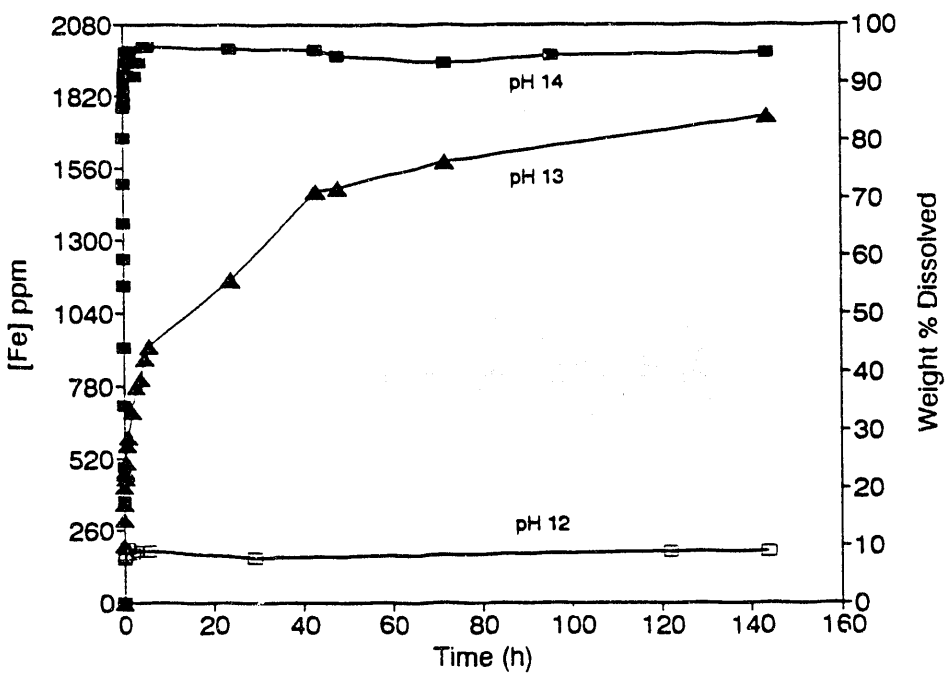

Figure 3.8. Solubility of Vendor-prepared $Na_2NiFe(CN)_6$ in NaOH as a Function of pH at 25°C, Extended Dissolution Time

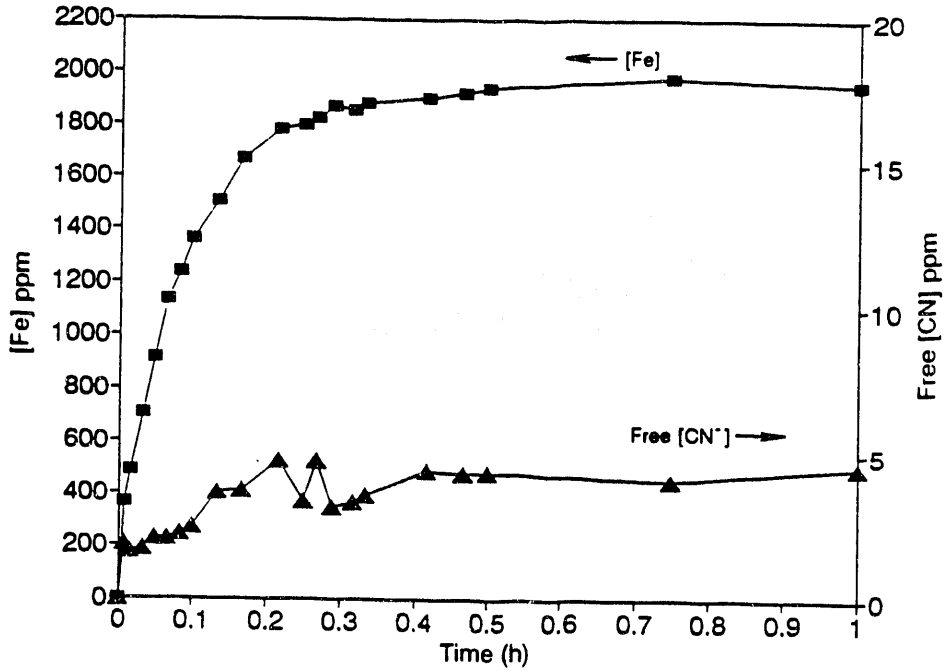

Figure 3.9. Soluble Iron and Free Cyanide in Solution vs. Time: Dissolution of Vendor-prepared $Na_2NiFe(CN)_6$ in 1.0 *M* NaOH

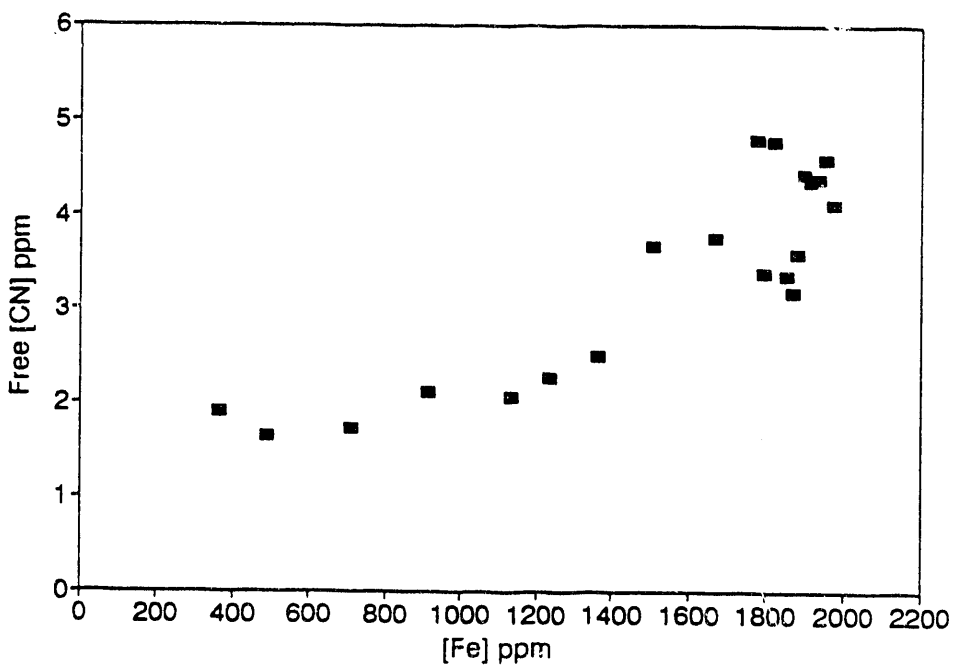

Figure 3.10. Plot of Free Cyanide vs. Soluble Iron: Dissolution of Vendor-prepared $Na_2NiFe(CN)_6$ in 1.0 *M* NaOH

3.2.2 Constant Ionic Strength Solution Experiments

Experiments were performed in which the sodium ion concentration was maintained at 1.0 *M* by addition of Na_2SO_4 to determine if the ionic strength of the solutions influenced the dissolution of sodium nickel ferrocyanide. Trends in solubility as pH is varied at 1.0 *M* [Na^+], shown in Figure 3.11, are similar to those observed in Figure 3.7 for solutions of different sodium ion concentrations. For experiments conducted at the same initial pH, the extent of dissolution tends to be lower at higher [Na^+], as shown in Figure 3.12 for 0.01 *M* NaOH (pH 12) and in Figure 3.13 for 0.1 *M* NaOH (pH 13). This may be a common ion effect.

3.2.3 SST Simulant Salt Experiments

In experiments to probe the influence of anions that would be present in the SSTs, a sample of the vendor-prepared material was dissolved in an aqueous solution of SST simulant salts to yield a solution with 1.0 *M* Na^+ concentration and a pH of 12.8. The solution was adjusted to pH 13.0 by addition of NaOH. The composition of the SST salt mixture is shown in Table 3.5.

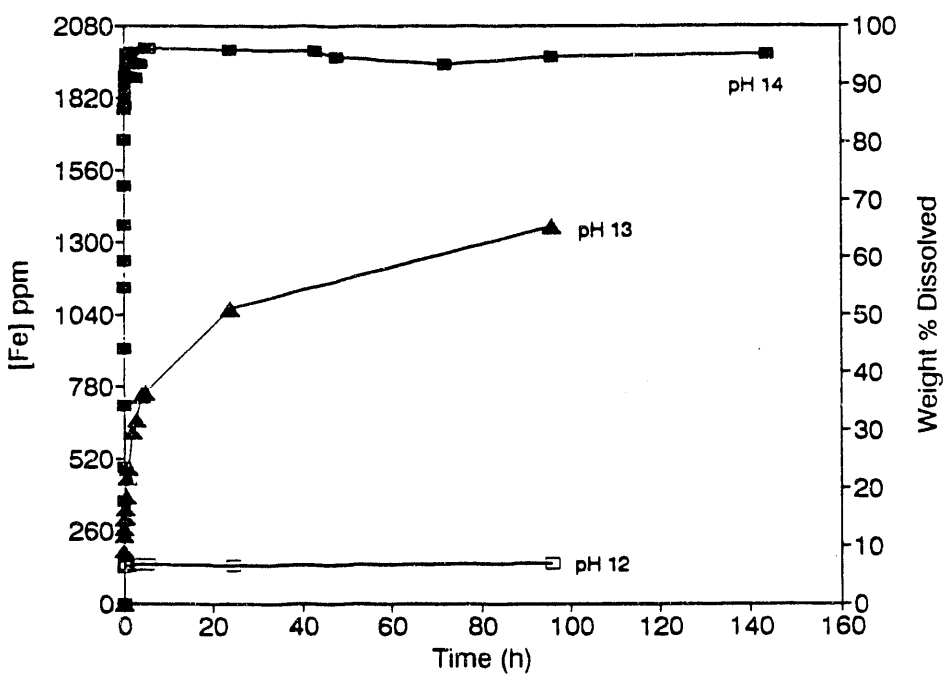

Figure 3.11. Dissolution of Vendor-prepared $Na_2NiFe(CN)_6$ in NaOH at 1 *M* [Na^+]

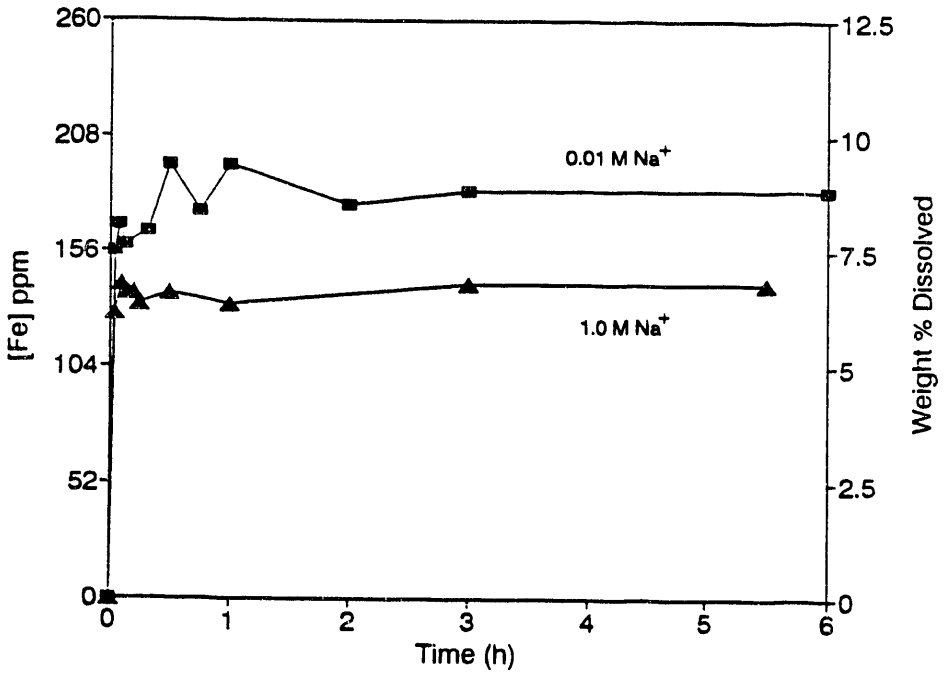

Figure 3.12. Effect of Sodium Ion Concentration on the Solubility of Vendor-prepared $Na_2NiFe(CN)_6$ at pH 12

Table 3.5. Composition of Single-shell Tank Simulated Salts

SST Component	Wt% Anhydrous
$NaNO_3$	80.47
$NaNO_2$	4.37
Na_2CO_3	1.52
NaOH	3.12
Na_2SO_4	1.48
Na_3PO_4	9.04

Figure 3.13 shows the rate of dissolution for this reaction mixture compared with that of the dissolution of the vendor-prepared $Na_2NiFe(CN)_6$ in pH 13 NaOH (0.1 *M* Na^+) and a pH 13 NaOH solution with Na_2SO_4 added to adjust the Na^+ concentration to 1.0 *M* (discussed in Section 3.2.2). Ferrocyanide dissolved faster in the pH 13 SST simulant salt solution than in either of the other pH 13 solutions; whereas addition of Na_2SO_4 suppressed dissolution, addition of SST salts enhanced dissolution. The rate enhancement was initially postulated to be the result of the precipitation of nickel phosphate, which is much less soluble than nickel hydroxide. However, analysis by IR, ESEM, EDS, and XRD could not substantiate the formation of nickel phosphate. (Nickel phosphate made in the laboratory was amorphous and did not give an XRD pattern.) The hydroxyl stretching absorption of $Ni(OH)_2$ appears in the IR spectrum and is thought to be the major nickel-containing product. The rate enhancement is probably caused by phosphate buffering, although the hydroxide ion concentration at the end of the reaction (13.0) is slightly greater than that of the buffer solution (pH 12.8 before pH adjustment to 13.0 with NaOH). The pH of the final SST solution was essentially unchanged; however, the pH of the comparable solution without SST salts dropped by 0.5 pH units.

Because the contents of actual SSTs are not being mixed, an experiment investigating the dissolution of the vendor-prepared $Na_2NiFe(CN)_6$ in the presence of SST simulant salts was conducted under static conditions. The experiment was conducted in Teflon labware at pH 13 with simulant salts added to give 1 *M* [Na^+]. To minimize disturbance, the solution was sampled less frequently (24-h intervals) than the stirred solutions. Prior to each sampling, a 5-s stirring was required to ensure a homogeneous solution phase. Figure 3.14 illustrates the rate of dissolution in the static experiment compared with dissolution in a stirred solution with the same initial composition. As expected, the rate of dissolution is slower in the static solution. Nevertheless, appreciable dissolution occurs. About 40% is dissolved after 24 h with no stirring and 90% dissolution is observed after 6 days. IC analysis for free cyanide ion shows 9.1 ppm after 72 h and 11.8 ppm after 144 h for samples protected from sunlight. Upon exposure to sunlight for 0.5 h, the 144-h sample contained 112 ppm free cyanide ion (9.5-fold increase), indicating the photosensitivity of these ferrocyanide solutions (Table 3.6).

3.3 Gamma Pit Dissolution Studies

Experiments were conducted to investigate the effect of gamma radiation on the dissolution of vendor-prepared $Na_2NiFe(CN)_6$. The Gamma Irradiation Facility (gamma pit) operated by PNL is located in the 3730 Building in the 300 Area. The facility contains 37 stainless steel irradiation tubes positioned in a 7-ft-diameter by 13.7-ft-deep stainless steel tank. Two arrays of ^{60}Co with a combined inventory of 32 KCi are located near the bottom of the tank. For radiation shielding purposes, the tank is completely filled with water. A concrete wall, 3.5 ft in height, surrounds the top of the tank. The irradiation tubes, which are sealed on the bottom, vary in length and diameter from 16 to 18 ft and 1.8 to 6 in., respectively. The irradiation flux of the tubes range from 2×10^6 R/h to 2×10^2 R/h. The uniform flux region varies from about 6 in. for the tubes closest to the sources to greater than 12 in. for the tubes farthest away from the sources. All flux measurements of the tubes are traceable to the National Institute of Standards and Technology.

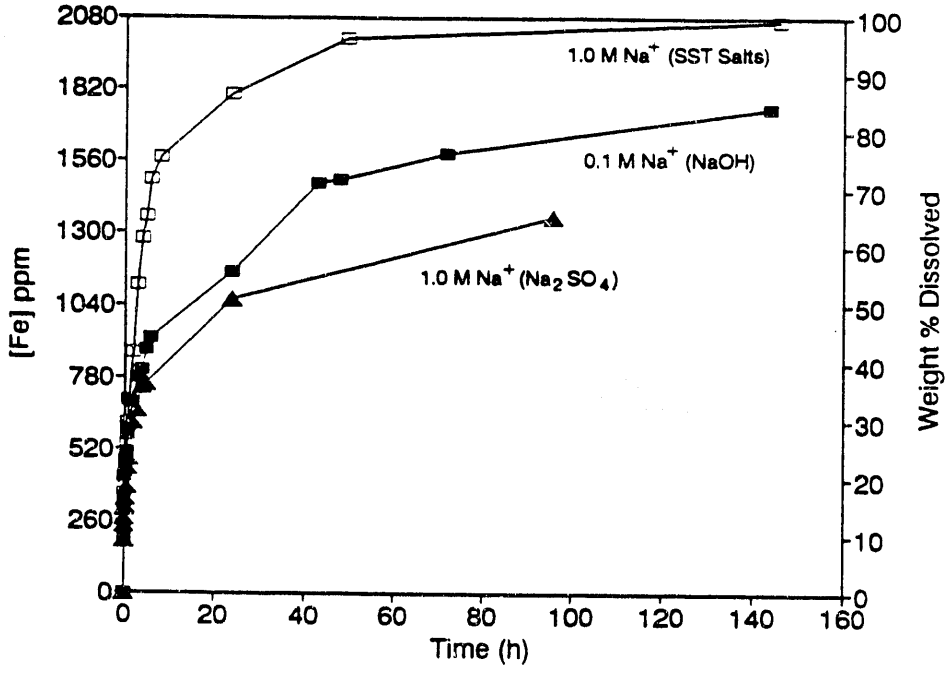

Figure 3.13. Dissolution of Vendor-prepared $Na_2NiFe(CN)_6$ in pH 13 Solutions Containing 1 *M* Na^+ from Single-shell Tank Salts (pH adjusted with NaOH); 1.0 *M* Na^+ from Na_2SO_4 and 0.1 *M* NaOH; and 0.1 *M* Na^+ from NaOH

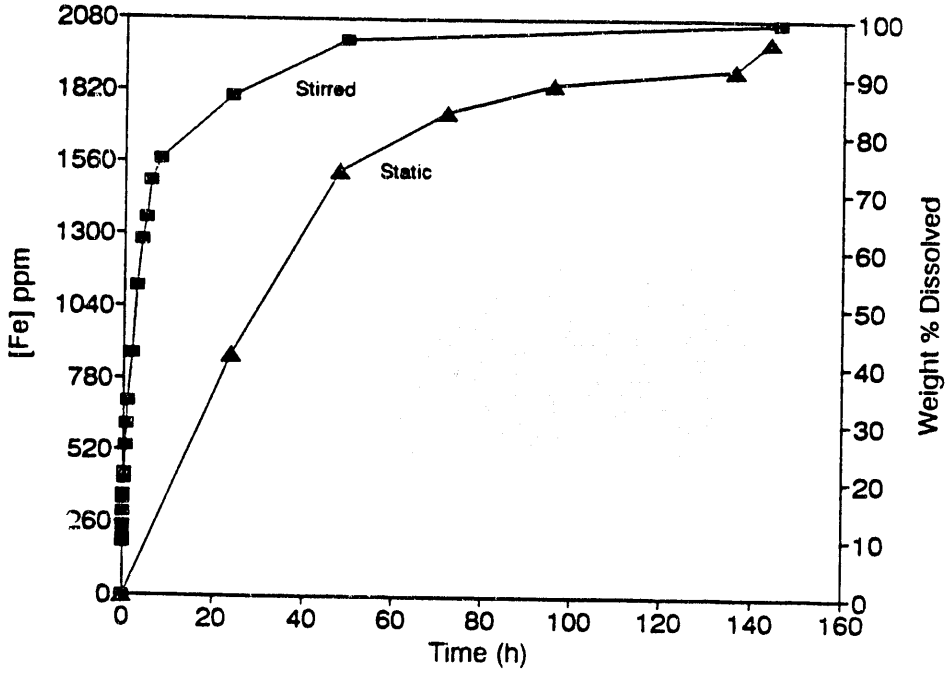

Figure 3.14. Comparison of Dissolution Behavior for Static and Stirred Solutions for Vendor-prepared $Na_2NiFe(CN)_6$ in SST Simulant Salt Solution at pH 13

Table 3.6. Concentrations of Free Cyanide Ion and Iron in Supernate Solutions (144-h Samples) Containing SST Simulant Salts

Experiment	[CN^-], ppm[(a)] Dark	[CN^-], ppm[(a)] Exposed	[Fe], ppm
SST Static	11.8	112.0	1898
Gamma-Irradiated	11.2	49.3	1291
Gamma Control	2.97	52.6	1291

(a) Dark solutions were protected from sunlight and analyzed. Exposed solutions were placed in sunlight for 0.5 h and re-analyzed.

Materials, capsules, and test systems are lowered into the irradiation tubes to the desired flux level manually or by using a half-ton crane. They are left in the tubes for a specific amount of time to attain the required exposure. There is no activation associated with the gamma irradiation so the materials can be transported to other facilities for examination after removal from the tubes.

Experimental conditions used in the gamma pit experiments were the same as those used in the SST simulant salt experiments (pH 13 and 1.0 *M* Na^+ by SST simulant salt addition) described in Section 3.2. Dissolution experiments were run at 25°C for 144 h without stirring. One reactor was placed in the gamma pit in a field of 1.65 x 10^5 R/h, while the other was placed outside of the pit as a control. Data from the static Teflon labware experiment served as a secondary baseline for the gamma pit experiments. Reaction vessels (stainless steel) and solutions were sparged with Ar/O_2 (80%/20%) prior to sealing in order to simplify mass spectrometry (MS) analysis and provide an atmosphere p[illegible]ed of nitrogen and CO_2, which could potentially be formed in these experiments. The initial pressure was 1 atmosphere.

Gas samples were taken at the conclusion of the experiments and analyzed by MS. Table 3.7 summarizes the results of MS analysis of gases produced in the reaction vessels. As expected, there was a greater amount of hydrogen produced in the gamma pit reaction vessel (1.30 x 10^{-4} moles) than in the control reaction vessel (2.57 x 10^{-6} moles).

The rate of dissolution of the vendor-prepared $Na_2NiFe(CN)_6$ material in the gamma pit was not monitored during the course of the reaction because of the logistics of obtaining samples from the reaction vessels. AA analyses were performed on supernates retrieved from the vessels at the end of the reaction. The final iron concentration was the same for both the gamma-irradiated and the control supernate solutions (1291 ppm), indicating that irradiation does not promote dissolution (Table 3.6). However, this value is lower than the solution iron concentration in the static SST simulant salt experiment (1898 ppm at 136 h). Infrared spectra of the insoluble solids (see below) suggest that the lower solution iron concentration may arise from re-precipitation of an iron cyanide species.

Table 3.7. Final Moles of Gas Present from the Gamma Pit Control and Irradiated Solutions

Gas	Final Moles of Gas		Irradiated/Control
	Control	Irradiated	
CO_2	7.33×10^{-7}	8.06×10^{-7}	1.10
$Ar^{(a)}$	2.83×10^{-3}	2.91×10^{-3}	1.03
$O_2^{(a)}$	7.22×10^{-4}	9.19×10^{-4}	1.27
N_2	1.11×10^{-4}	7.42×10^{-5}	0.67
H_2	2.57×10^{-6}	1.30×10^{-4}	50.58
CO	3.67×10^{-6}	4.03×10^{-6}	1.10
He	BDL[(b)]	BDL	-
CH_4	BDL	BDL	-
N_2O	BDL	BDL	-
NO_x	BDL	BDL	-

(a) Initial moles: Ar, 2.93×10^{-3}; O_2, 7.55×10^{-4}.
(b) BDL = Below Detection Limits (<0.01 vol%).

IC was used to determine the amounts of free cyanide, ferrocyanide, and ferricyanide in the gamma-irradiated and control supernate solutions. Ferrocyanide was the primary species identified in the analyses. No ferricyanide was observed. A small unidentified shoulder, presumably arising from an iron cyanide species, was noted in all of the chromatograms. Free cyanide analysis by IC, Table 3.6, showed that more cyanide was liberated in the gamma-irradiated sample (11.2 ppm free cyanide) than in the control (2.97 ppm free cyanide).

The supernates were susceptible to a rapid photolysis reaction in which the light yellow solutions exposed to sunlight turned deep yellow. Samples of the supernates exposed to sunlight showed the iron cyanide content was unchanged. However, like the static SST experiment conducted in Teflon labware, there was a sizable increase in the concentration of free cyanide in the solutions (Table 3.6). The free cyanide concentration in the exposed gamma-irradiated supernate was 49.3 ppm (4.4-fold increase), and the exposed control sample was 52.6 ppm (17.7-fold increase).

Infrared spectra, in the cyanide region, of solids obtained from the supernates were the same as those of samples from other dissolution experiments (Table 3.4). The ESEM/EDS, as before, indicated that nickel is not present in solution and that most of the iron is found in these soluble solids. However, the SST salts in this fraction were too concentrated to allow for identification of a ferrocyanide phase by XRD.

Figure 3.15 illustrates the cyanide infrared absorbance region of the insoluble solids for the two gamma pit experiments and the static SST experiment (see also Table 3.4). The cyanide absorbances are more complex for solids from the gamma pit experiments than those from the SST experiment. Each of the gamma pit spectra have similar vibrational bands but with differing intensities. It is apparent that these materials contain more than one iron cyanide compound. Each contains undissolved $Na_2NiFe(CN)_6$. While this compound appears to be the major cyanide-containing component of the SST stirred reaction insoluble solids and of the pH variation (non-SST) insoluble solids, it is a

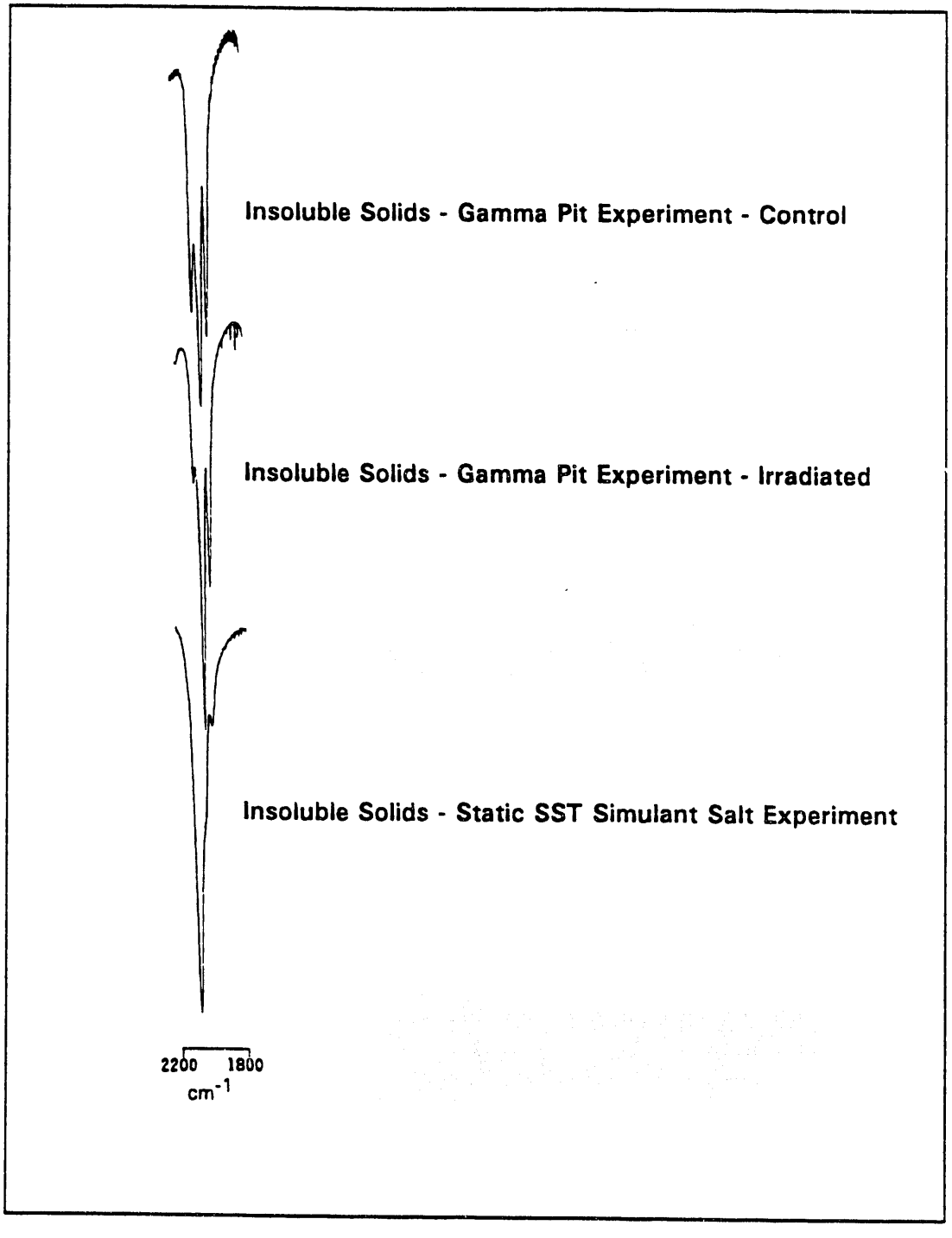

Figure 3.15. IR Spectra in the Cyanide Region of Insoluble Solids from Gamma Pit and SST Experiments

minor component of the gamma-irradiated and control materials. The major cyanide-containing component of the insoluble solids in the control experiment is not the major component of the irradiation experiment. The identity of these species is unknown at this time but one may be $Na_3Fe(CN)_5(H_2O)$, a cyanide substitution product. Another possibility is iron ferrocyanide if cyanide leaches iron out of the stainless steel reactor.

Overall, the insoluble solids consist primarily of $Ni(OH)_2$. This is clearly shown in XRD and IR spectra. A small amount of nitrate is also identified, but a ferrocyanide phase is not detectable by the XRD method. The iron concentration is very low as indicated by weak signals obtained by Mössbauer spectroscopy (Figure 3.16). However, the spectrum clearly shows that two iron species are present; one is most likely ferrocyanide (peak at -0.19 mm/s), while the other is unidentifiable but is not ferricyanide.

Ferricyanide is absent in both soluble and insoluble recovered solids. This absence was unexpected because of the known reaction of ferrocyanide with hydroxyl radical, which is formed in the gamma field, to produce ferricyanide (Maliyackel et al. 1990). This oxidation may be suppressed by the presence of nitrite anion, which also reacts with hydroxyl radical.

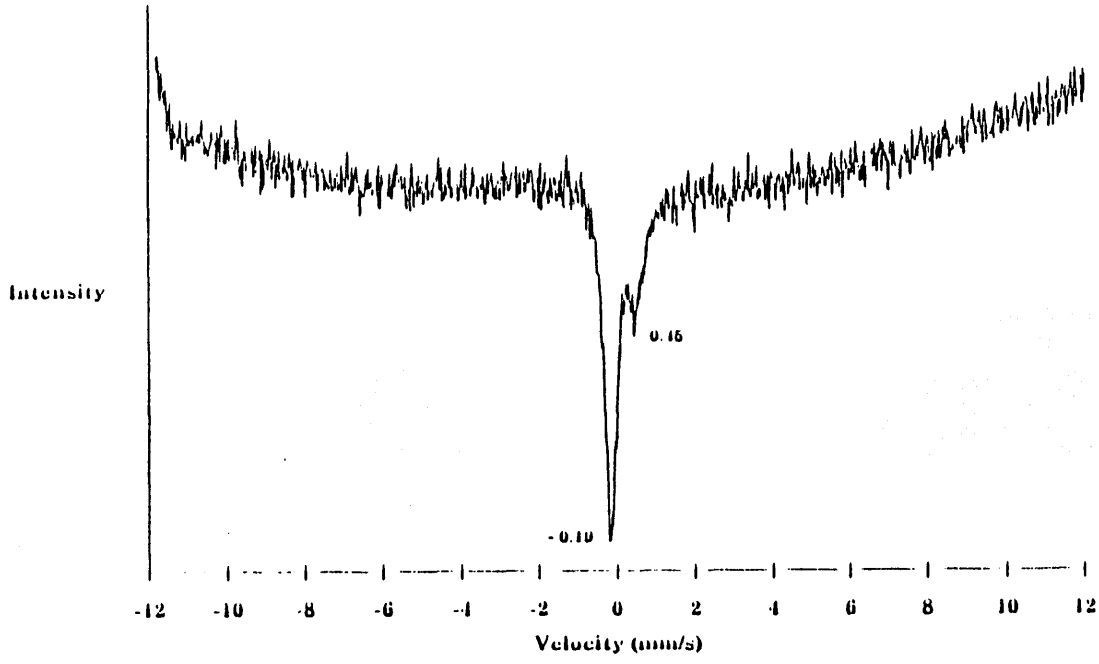

Figure 3.16. Mössbauer Spectrum of the Insoluble Solids Obtained from the Gamma-irradiated Solution

4.0 Conclusions

Vendor-prepared $Na_2NiFe(CN)_6$ dissolves in aqueous base to give soluble and insoluble products. Insoluble solids obtained from dissolution experiments consist primarily of $Ni(OH)_2$ with small amounts of undissolved starting material. Precipitation of $Ni(OH)_2$ apparently drives the ferrocyanide dissolution. From the gamma pit experiments, the insoluble solids contained more than one iron cyanide species, yet to be identified. The primary cyanide-containing component of the soluble solids is $Na_4Fe(CN)_6$.

The rate of dissolution of vendor-prepared $Na_2NiFe(CN)_6$ in aqueous base is rapid, increasing as the pH increases from 12 to 14. At pH 14, 95% dissolution is observed after 0.5 h. Addition of 1 *M* Na^+ ions in the form of Na_2SO_4 suppresses dissolution at pH 13, presumably because of a common ion effect. However, 1 *M* Na^+ in the form of SST simulant salts (sodium salts of phosphate, carbonate, nitrate, nitrite, sulfate, and hydroxide) resulted in an enhancement of the rate of solubilization. Because the pH of the SST salt solution does not change through the course of the reaction and the major insoluble product is $Ni(OH)_2$, the rate enhancement most likely arises from buffering of the solution by phosphate. Even when the solution is not stirred, dissolution is relatively rapid. Approximately 40% of the $Na_2NiFe(CN)_6$ dissolves in 24 h in an unstirred solution containing SST salts.

Gamma radiation does not appear to greatly affect the dissolution reaction. Similar rates were observed in unstirred irradiated and control solutions. However, the extent of reaction in these experiments is lower than that in a static experiment conducted in Teflon labware. The more complex mixture of iron cyanides in the insoluble fraction of the gamma pit dissolution studies suggests the possibility that an iron cyanide species re-precipitates from solution. Further work is needed to determine whether iron is leached from the reaction vessels and precipitates ferric ferrocyanide or whether some other process is occurring. The effect of gamma radiation on cyanide or ferrocyanide hydrolysis was not determined but is a subject to be investigated during FY 1993.

5.0 Future Work

Solubilization experiments will be completed in FY 1993. The temperature dependence of the dissolution of vendor-prepared $Na_2NiFe(CN)_6$ in aqueous base will be investigated. An experiment at a higher sodium ion concentration (6 *M* Na^+ as the sulfate or nitrate) will be conducted. Results of an experiment at an initial pH of 14 (out of the buffer region for phosphate) with 1 *M* Na^+ as SST salts compared with the complementary experiment without SST salts will give further information about the role of anions in the dissolution. Similar results in these two experiments would indicate that buffering is the likely cause of the rate enhancement observed at pH 13. Dissolution in the presence of Na_3PO_4 (non-SST) at pH 13 will also give information about buffering. A gamma pit experiment on solutions not containing SST salts is planned in order to study dissolution in unbuffered solutions. The effect of stainless steel on the course of the solubilization reactions will be probed. In addition, flowsheet materials prepared in FY 1992 by WHC will be investigated.

Cyanide and ferrocyanide hydrolysis studies will be conducted. The effects of high ionic strength and gamma radiation are of interest.

6.0 References

Borsheim, G. L., and B. C. Simpson. 1991. An Assessment of the Inventories of the Ferrocyanide Watchlist Tanks. WHC-SD-WM-ER-133 Rev. 0, Westinghouse Hanford Company, Richland, Washington.

Burger, L. L. 1984. Complexant Stability Investigation, Task 1 - Ferrocyanide Solids. PNL-5441, Pacific Northwest Laboratory, Richland, Washington.

Burger, L. L., and R. D. Scheele. 1988. Interim Report - Cyanide Safety Studies. PNL-7175, Pacific Northwest Laboratory, Richland, Washington.

Burger, L. L., and R. D. Scheele. 1991. The Reactivity of Cesium Nickel Ferrocyanide Towards Nitrate and Nitrite Salts - A Status Report. PNL-7550, Pacific Northwest Laboratory, Richland, Washington.

Burger, L. L., D. A. Reynolds, W. W. Schultz, and D. M. Strachan. 1991. A Summary of Available Information on Ferrocyanide Tank Wastes. PNL-7822, Pacific Northwest Laboratory, Richland, Washington.

Maliyackel, A. C., W. L. Waltz, J. Lilie, and R. J. Woods. 1990. "Radiolytic Study of the Reactions of Hydroxyl Radical with Cobalt(III), Iron(II), and Ruthenium(II) Complexes Containing 2,2'-Bipyridal and Cyano Ligands." Inorganic Chemistry 29:340-348.

Nakamoto, K. 1970. Infrared Spectra of Inorganic and Coordination Compounds, 2nd Edition. Wiley-Interscience, New York.

Peach, J. D. 1990. "Consequences of Explosion of Hanford's Single-Shell Tanks are Underestimated." Letter B-241479 dated October 1990 to M. Synar, GAO/RCED-91-34, General Accounting Office, Washington, D.C.

Scheele, R. D., L. L. Burger, J. M. Tingey, S. A. Bryan, G. L. Borsheim, B. C. Simpson, R. J. Cash, and H. H. Cady. 1991. Ferrocyanide-Containing Waste Tanks: Ferrocyanide Chemistry and Reactivity. PNL-SA-19924, Presented at Environmental Restoration 1991, Pasco, Washington.

U.S. Department of Energy (DOE). 1987. Final Environmental Impact Statement, Disposal of Hanford Defense High-Level, Transuranic, and Tank Wastes. DOE-EIS-0113, Washington, D.C.

U.S. Department of Energy (DOE). 1990. "DOE to Develop Supplemental Environmental Impact Statement for Hanford." Press Release, October 9, 1990, Washington, D.C.

PNL-8387
UC-721

Distribution

No. of Copies

OFFSITE

12 DOE Office of Scientific and Technical Information

25 John C. Tseng
U.S. Department of Energy
EM-35, Trevion II
Washington, D.C. 20585

P. Gene Woodall
U.S. Department of Energy
Idaho Operations Office
785 DOE Place
Idaho Falls, Idaho 83402

Thomas C. Temple
U.S. Department of Energy
Savannah River Operations Office
P.O. Box A
Aiken, South Carolina 29808

5 Charles S. Abrams
1987 Virginia
Idaho Falls, ID 83404

David O. Campbell
102 Windham Road
Oak Ridge, TN 37830

Fred N. Carlson
6965 North 5th West
Idaho Falls, ID 83401

Donald T. Oakley
409 12th Street SW, Suite 310
Washington, DC 20024-2188

No. of Copies

Arlin K. Postma
3640 Ballard Road
Dallis, Oregon 97338

William R. Prindle
1556 Crestline Drive
Santa Barbara, CA 93105

Alfred Schneider
5005 Hidden Branches Drive
Dunwoody, GA 30338

George E. Schmauch
Air Products & Chemicals
7201 Hamilton Blvd.
Allentown, PA 18195-1501

James A. Gieseke
Battelle Columbus Division
555 King Avenue
Columbus, OH 43201-2693

Kamal K. Bandyopadhyay
Brookhaven National Laboratory
Upton, NY 11973

Morris Reich
Brookhaven National Laboratory
Upton, NY 11973

Gary Powers
Design Science, Inc.
163 Witherow Road
Sewickley, PA 15143

William C. Schutte
EG and G Idaho, Inc.
P.O. Box 1625
Idaho Falls, Idaho 83415

No. of
Copies

Hans K. Fauske
Fauske and Associates, Inc.
16W070 W. 83rd St.
Burr Ridge, IL 60521

Gregory R. Choppin
Florida State University
Department of Chemistry B-164
Tallahassee, FL 32306

Melvin W. First
Harvard University
295 Upland Avenue
Newton Highlands, MA 02161

Chester Grelecki
Hazards Research Corporation
200 Valley Road, Suite 301
Mt. Arlington, NJ 07856

Billy C. Hudson
Lawrence Livermore National
Laboratory
P.O. Box 808, L-221
Livermore, CA 94550

Steve F. Agnew
Los Alamos National Laboratory
P.O. Box 1663
Los Alamos, NM 87545

Steve Eisenhawer
Los Alamos National Laboratory
P.O. Box 1663
Los Alamos, NM 87545

Thomas E. Larson
Los Alamos National Laboratory
P.O. Box 1663
Los Alamos, NM 87545

No. of
Copies

Harold Sullivan
Los Alamos National Laboratory
P.O. Box 1663
Los Alamos, NM 87545

Mujid S. Kazimi
MIT/Dept of Nuclear Eng.
77 Massachusetts Avenue
Room 24-102
Cambridge, MA 02193

Louis Kovach
NUCON
P.O. Box 29246
Columbus, OH 43229

Emory D. Collins
Oak Ridge National Laboratory
P.O. Box 2008
7930, MS-6385
Oak Ridge, TN 37831-6385

Charles W. Forsberg
Oak Ridge National Laboratory
105 Mitchell Road
MS-6495
Oak Ridge, TN 37831-6495

Thomas S. Kress
P.O. Box 2009, MS-8088
Oak Ridge, TN 37831-8088

David J. Pruett
P.O. Box 2008
Building 4501, MS-6223
Oak Ridge, TN 37831

Andrew S. Velentsos
Rice University
5211 Paisley
Houston, TX 77069

No. of Copies

Scott E. Slezak
Sandia National Laboratory
P.O. Box 5800
Albuquerque, NM 87185

3 Ray S. Daniels
Science Applications International Corporation
12850 Middlebrook Road
Trevion I, Suite 300
Germantown, MD 20874

John M. Saveland
Science Applications International Corporation
12850 Middlebrook Road
Trevion I, Suite 300
Germantown, MD 20874

Joseph S. Byrd
University of South Carolina
Department of Electrical and Computer Engineering
Swearingen Engineering Center
Columbia, SC 29208

Bruce R. Kowalski
University of Washington
Center for Process Analytical Chemistry
Chemistry Department BG-10
Seattle, WA 98195

Frank L. Parker
Vanderbilt University
P.O. Box 1596, Station B
Nashville, TN 37235

David K. Ploetz
West Valley Nuclear Services Co., Inc.
Rock Springs Road (Box 191)
West Valley, New York 14171

No. of Copies

Alan P. Hoskins
Westinghouse Idaho Nuclear Co., Inc.
1955 Freemont Avenue
P.O. Box 4000
Idaho Falls, Idaho 83403-4000

Paul d'Entremont
Westinghouse Savannah River Company
P.O. Box 616, 703-H
Aiken, South Carolina 29802

ONSITE

12 DOE Richland Field Office

R. F. Christensen (8), A4-02
R. E. Gerton, A4-02
A. G. Krasopoulos, A5-55
Public Reading Room, A1-65
RL Docket File, A3-11

68 Westinghouse Hanford Company

J. M. Atwood, SO-61
H. Babad, R2-31
D. B. Bechtold, T6-50
J. B. Billetdeaux, R2-08
G. L. Borsheim, R2-11
V. C. Boyles, R1-49
R. J. Cash (10), R2-31
M. D. Crippen, H5-32
R. D. Crowe, B4-55
C. DeFigh-Price, B4-55
D. R. Dickinson, R2-32
G. T. Dukelow (2), R2-32
J. G. Flandro, R2-31
C. J. Forbes, R1-08
K. D. Fowler, R2-11
G. L. Fox, L5-01
G. T. Frater, R2-31
J. C. Fulton, R2-31
K. A. Gasper, R2-08

No. of Copies

J. M. Grisby, H5-32
T. W. Halverson, T5-49
D. G. Hamrick, R2-31
H. D. Harmon, R2-52
D. L. Heer, H0-38
J. D. Hopkins, R2-08
R. D. House, R2-83
L. L. Humphreys, R2-52
M. N. Islam, R3-08
D. W. Jeppson, L5-31
J. R. Jewett, T6-50
N. W. Kirch, R2-11
W. L. Knecht, H0-34
C. A. Kuhlman, B3-30
J. D. McCormack, L5-31
J. M. McLaren, H0-34
N. J. Milliken, H5-34
A. F. Noonan, R2-12
R. S. Popielarczyk, R1-30
J. G. Propson, R2-18
R. E. Raymond, R1-80
I. E. Reep, R2-08
E. L. Renner, R2-08
D. A. Reynolds, R2-11
D. C. Richardson, R2-31
C. P. Schroeder, L7-06
M. H. Shannon, H5-30
N. L. Simon, R2-78

No. of Copies

B. C. Simpson, R2-12
H. Toffer, H0-38
D. D. Wodrich, R2-23
R. K. Welty, R1-80
W. F. Zuroff, R2-14
Document Processing and Distribution (2), L8-15
Central Files, L8-04
EDMC, H4-22
Information Release Administration, A2-24
TFIC, R1-28

22 Pacific Northwest Laboratory

R. T. Allemann, K7-15
S. A. Bryan, P7-25
R. T. Hallen, P8-38
B. M. Johnson (3), K1-78
M. A. Lilga (5), P8-38
M. R. Lumetta, P8-38
R. A. Romine, P8-38
R. D. Scheele, P7-25
G. F. Schiefelbein, P8-38
D. M. Strachan, K2-38
Publishing Coordination
Technical Report Files (5)

END

DATE FILMED

3 / 17 / 93